Impact of vegetation greening on carbon and water cycle in the African Sahel-Sudano-Guinean region

Booker O. Ogutu[1*], Francesco D'Adamo[1] and Jadunandan Dash[1]

[1]School of Geography and Environmental Science, University of Southampton, Highfield, Southampton, SO17 1BJ, United Kingdom

Abstract

The African Sahel-Sudano-Guinean region is one of the largest water limited environments in the world, thus making it highly vulnerable to climate change. Recent studies have shown vegetation greening in the region, but few have investigated the impact of this greening on carbon and water cycles. We used a combination of earth observation (EO) data and a diagnostic model to evaluate the extent of the vegetation greening and its impacts on carbon sequestration potential (i.e., Gross Primary Productivity-GPP) and the water cycle (i.e., Evapotranspiration-ET and Water Use Efficiency-WUE) from 1982 to 2015. Additionally, we evaluated the influence of key climatic variables (i.e., precipitation, temperature, and solar radiation) on vegetation greening, carbon sequestration potential and the water cycle. Our results showed widespread vegetation greening during the first half of the study period (1982-2000), driven mainly by increase in precipitation. However, the rate of greening reduced or became stagnant during the latter half of the study (2000-2015), but did not revert to pre-greening levels of 1980s, implying a persistent ecosystem change. The vegetation greening and increased precipitation resulted in a *~17.95%* increase in GPP (from *~3.9 PgC/year* in 1982 to *~4.6 PgC/year* in 2000) and a *~21.28%* increase in ET (from *~47 mm/year* in 1982 to *~57 mm/year* in 2015). The WUE showed an overall reduction, mainly attributed to large increases in ET not matched by similar magnitude of increases in GPP. Currently, there is lack of consensus on the magnitude of the contribution of drylands to the global carbon and water

cycle. This study shows that drylands undergoing ecosystem change, coupled with climate change, may in future become important contributors to the global carbon and water cycle. Therefore, they could play a key role in future global warming and climate change mitigation strategies.

Keywords: *Vegetation greening*, *Water use efficiency, Carbon sequestration, SCARF model, Gross primary productivity*

*Corresponding Author: B.O.Ogutu@soton.ac.uk

1. Introduction

The African Sahel-Sudano-Guinean region is one of the main drylands of the world and is considered to be highly vulnerable to climate change and anthropogenic activities (Kaptue et al., 2015). In the 1970s and 1980s the region was hit by several severe droughts that resulted in famines, killing up to 100,000 people (Ibrahim, 1988, Kandji *et al.,* 2006). The frequent occurrence of these droughts coupled with local-scale studies on environmental degradation in the early parts of the 20th century (Sinclair and Fryxell, 1985) led to the hypothesis that desertification was expanding southwards of the Sahara Desert (UNCOD, 1977; Sinclair and Fryxell, 1985). However, in the 1990s this notion began to be challenged after evidence started to emerge showing vegetation re-greening (increase in green cover) and lack of any large-scale desertification (Thomas and Middleton, 1994; Prince et al., 1998; Nicholson et al., 1998). In the recent past, several studies using Earth Observation (EO) data have demonstrated that the Sahel region has in fact, been experiencing vegetation re-greening since the early 1990s (Ekludh and Olsson, 2003; Hickler et al., 2005; Olsson et al., 2005; Hermann et al., 2005; Fensholt et al., 2012; Dardel et al., 2014; Kaptue et al., 2015). This re-greening has been attributed to several factors including: wetter climatic conditions (Haarsma et al., 2005; Kaptue et al., 2015; Brandt et al., 2016), CO_2 fertilisation due to increased CO_2 in the atmosphere (Bathiany et al., 2014; Traore et al., 2014; Lu et al., 2016), and increase in woody vegetation (Brandt et al., 2015; Brandt et al., 2016, Venter et al., 2018; Anchang et al., 2019). Even though the vegetation re-greening has dispelled the notion of expansion of desertification, it is still argued that it may not necessarily lead to optimal ecosystem function and services (Hein and Ridder, 2006; Hermann and Tappan, 2013; Ibrahim et al., 2018). For example, re-greening driven by alteration of vegetation structure and species composition (e.g., through encroachment of invasive species), may lead to loss of biodiversity and ecosystem service provision (Hein and Ridder, 2006; Hermann and Tappan, 2013; Ibrahim et al., 2018).

Since the Sahel-Sudano-Guinean region is mainly characterised by seasonal dry conditions, the changes in its ecosystem through vegetation greening is likely to influence its carbon sequestration potential and water cycle. This is because terrestrial carbon sequestration and water cycle are tightly coupled in drylands as precipitation and drought are the key drivers of primary production, while vegetation dynamics on the other hand exerts strong controlling effects on water circulation (Tietjen et al., 2010). Additionally, the African Sahel-Sudano-Guinean region is predicted to become warmer, and its precipitation regime altered (i.e., some models predict increase in precipitation while others predict reduction in precipitation) as a result of climate change (Kent et al. 2015, Rowell et al., 2016). These shifts due to climate change, coupled with vegetation greening, could lead to changes in the carbon sequestration potential and water cycle of the region and its contribution to the global carbon and water cycle.

Until recently, the role of terrestrial dryland ecosystems in the global carbon and water cycle was considered insignificant. However, seminal studies by Poulter et al., (2014) and Ahlstrom et al., (2015) found that drylands were dominant contributors to the global carbon sink changes over time (contributing up to 57% or 0.04 PgC $year^{-1}$ of the global 0.07 PgC $year^{-1}$ positive trend in the global carbon sink) (Ahlstrom et al., 2015). Additionally, southern hemisphere drylands in particular were found to play a major role in driving the inter-annual anomaly of terrestrial ecosystems global carbon sinks (Poulter et al., 2014). However, there is still lack of consensus on the magnitude of the contribution drylands to the global carbon sink, whether drylands can act as long-term carbon sinks (e.g., due to frequent occurrence of extreme climatic events such as droughts in these regions resulting in depletion of vegetation and enhanced decomposition of organic matter) and the impacts of ecosystem changes such as vegetation re-greening on their carbon sequestration potential. Therefore, the observed vegetation re-greening in the Sahel-Sudano-Guinean region offers an opportunity to understand how such

changes, coupled with climate change, affect the carbon sequestration potential of dryland ecosystems and ultimately the global carbon cycle.

As carbon and water cycle are tightly coupled in drylands, changes in vegetation structure through re-greening is likely to have an impact on the water cycle, for example, through the alteration of evapotranspiration-ET and water use efficiency-WUE. Ecosystem WUE, defined as the ratio between vegetation productivity (quantified as GPP) and ecosystem water loss through ET (Keenan et al., 2013; Huang et al., 2015; Yang et al., 2016; Cheng et al., 2017; Zheng et al., 2019), has been recognised as an important indicator of how ecosystems respond and adapt to environmental and climate change (Keenan et al., 2013; Cheng et al., 2017; Zhou et al., 2017). A reduction in WUE can be equated to degradation of an ecosystem, while an increase in WUE can be an indicator of ecosystem resilience (Kaptue *et al.,* 2015; Liu et al., 2015). Recent global scale studies have reported that increases in atmospheric carbon dioxide due to anthropogenic activities and regreening can lead to increases in an ecosystems water use efficiency (Keenan et al., 2013; Cheng et al., 2017; Zhou et al., 2017). However, few regional studies have investigated the impact of the observed vegetation re-greening and climate change on the water cycle (i.e., WUE and ET) in the African Sahel-Sudano-Guinean region.

Therefore, the aim of this study was to understand the impact of vegetation greening in the Sahel-Sudano-Guinean region on its carbon sequestration potential (represented by gross primary production-GPP) and water cycle (represented by ET and WUE). Additionally, the study investigated the role of various climatic drivers (i.e., precipitation, temperature and solar radiation-represented by photosynthetically active radiation-PAR) on the dynamics of vegetation greening, GPP, ET and WUE in the region. To achieve the aim of this study, the following questions were investigated: 1) What was the spatial-temporal dynamics of vegetation greening, GPP, ET and WUE in the region, 2) What was the relationship between vegetation greening and trends in GPP, ET, and WUE, and 3) What was the influence of various

120 climatic variables (i.e., precipitation, temperature, and PAR) on the trends of vegetation
121 greening, GPP, ET and WUE.

122

123 **2. Materials and Methods**

124 **2.1. Study Area**

125 The geographic extent of the African Sahel-Sudano-Guinean region stretches from the Atlantic
126 Ocean in the west to the Red Sea and parts of the Indian Ocean to the East (Figure 1). The
127 region is characterised by arid, semi-arid, dry sub-humid, and humid conditions. The northern
128 parts bordering the Sahara Desert has a mean annual rainfall of less than 100 mm. The southern
129 parts are composed of dry sub-humid savannas, woodlands, and evergreen forests, with annual
130 rainfall ranging from 600-1000 mm (Nicholson, 2013; Abdi et al., 2014). The climatic system
131 of the western parts is driven mainly by the West African monsoon, which brings rain from
132 May to October (Nicholson, 2009). The eastern parts have its climate mostly controlled by the
133 dynamics of Sea Surface Temperature (SST) over the Equatorial Pacific and Indian Ocean
134 (Endris et al., 2019). The rainfall pattern exhibits high rates of spatial variability, which often
135 lead to significant variability in water availability and drought events (Ali and Lebel 2009).
136 The Sahel-Sudano-Guinean region is home to more than half a billion people and the main
137 economic activity of most of the rural inhabitants in the region include livestock pastoralism
138 in the drier northern regions and subsistence agriculture in the wetter southern regions (Neely
139 et al., 2009). The northern regions are less densely populated (i.e., approximately 2.6 persons
140 per Km^2 in the Sahel sub-region), whereas the southern regions are more densely populated
141 (i.e., approximately 99 persons per Km^2 in the Guinean region) (Herrmann et al., 2020).

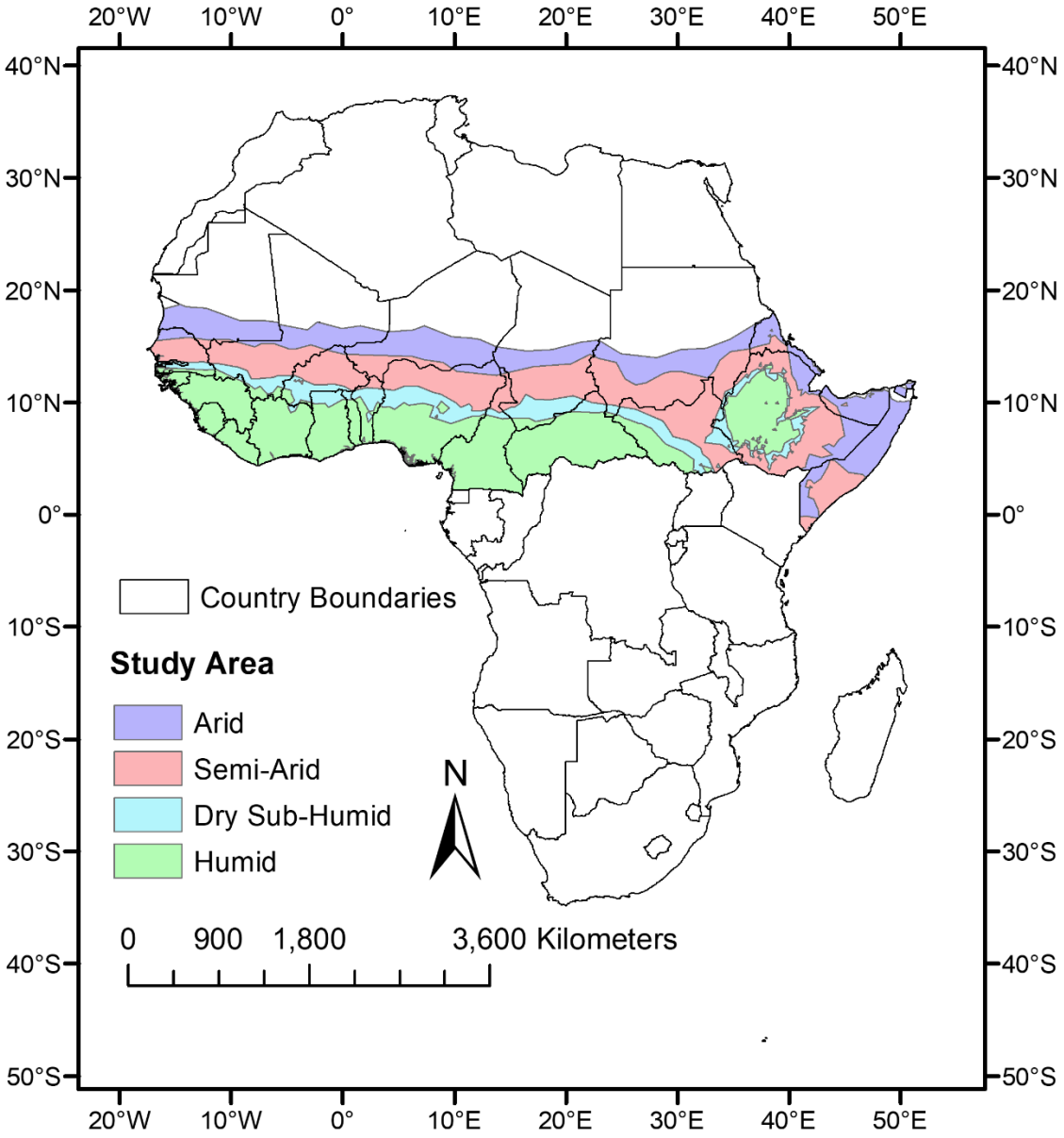

142

143 *Figure 1: The extent of the study area (i.e., Sahel-Sudano-Guinean region) with superimposed*

144 *climatic/aridity zones (Source: FAO Aridity Index zones)*

145 **2.2. Data description**

146 *2.2.1. Normalised difference vegetation index*

147 To evaluate the spatial extent and trends in vegetation greening, we used the latest version of

148 the Global Inventory Modelling and Mapping Studies (GIMMS) Normalised Difference

149 Vegetation Index (NDVI) data (i.e., GIMMS NDVI3g.v1) covering the period from July 1981
150 to December 2015 (*https://ecocast.arc.nasa.gov/data/pub/gimms/3g.v1/*). The data is provided
151 at 8 km spatial resolution and composited at 15-day time step. It has been corrected for sensor
152 degradation, sensor calibration, varying sensor view geometry and impacts of volcanic aerosols
153 (Pinzón et al., 2005; Pinzon and Tucker, 2014). To ensure only good quality data was used, we
154 consulted the quality control flags and used only those pixels categorised as having the best
155 quality (Flag0). Additionally, we masked out pixels that represent non-vegetated surfaces (i.e.,
156 NDVI<0.1). We used 0.1 threshold as it resulted in the lowest loss of pixels and has been
157 reported in previous studies to successfully mask out non-vegetated pixels (Bi et al., 2013).
158 The 15-day maximum value composite (MVC) NDVI data were then averaged to monthly
159 composites and eventually to annual means. The data was first averaged to monthly means in
160 order to allow for checking of the consistency of the annual means. When averaging monthly
161 data to annual means, the ideal scenario was for each pixel to have 12 months of valid NDVI
162 values. However, this was not always the case, therefore, we run a sensitivity analysis to
163 determine the minimum number of months required to achieve a representative annual mean
164 value. The sensitivity analysis was done by first selecting those pixels with 12-months of good
165 quality data. We then randomly removed months from the data and calculated the difference
166 between the mean obtained with the full and reduced number of months. We set the minimum
167 number of months to be used in the calculating annual mean as the number of months where
168 the average difference between the mean from the full 12 months data and the reduced months
169 data was ≤5%. Based on this sensitivity analysis, a minimum of 10 months of data was required
170 to achieve representative annual mean and therefore, annual means were only calculated for
171 those pixels with a minimum of 10 valid monthly NDVI values.

172 *2.2.2. Gross Primary Production*

To evaluate the dynamics of carbon sequestration potential we generated gross primary production (GPP) estimates from 1982 to 2015 using the Southampton Carbon Flux (SCARF) Model (Ogutu et al., 2013; Chiwara et al., 2018). The SCARF model is a light use efficiency (LUE) model with the added advantage of exploiting the intrinsic quantum yield of the two dominant photosynthetic pathways in plants (i.e., C_3 and C_4). The SCARF model derives GPP as a function of Photosynthetic Active Radiation-PAR, the Fraction of Photosynthetic Active Radiation absorbed by photosynthetic elements in the canopy (FAPARps), Quantum yield for either C_3 or C_4 plants and photosynthesis limiting factors (i.e., vapour pressure deficit and air temperature) (See detail SCARF Model description in Supplementary Material).

The SCARF model was driven by a number of datasets (i.e., Land Cover, Solar Radiation, Air Temperature, Vapour Pressure Deficit, and Fraction of Absorbed Photosynthetically Active Radiation-FAPAR) (Supplementary Material, Table S1) to produce GPP in gC/m^2 at monthly time-steps. These were then aggregated to annual time-steps for further analysis. The output from the model was validated using GPP data from Flux tower sites located in the study area (Supplementary Material). We used the Level 4 monthly GPP data, which was gap filled using the Marginal Distribution Sampling (MDS) method described in Reichstein et al. 2005, in order to ensure consistency with the GPP model simulation time-step.

2.2.3 Evapotranspiration

To evaluate the dynamics of in evapotranspiration (ET) we used data generated by the National Terradynamic Simulation Group (NTSG), University of Montana (*http://files.ntsg.umt.edu/data/ET_global_monthly/*). The ET data is provided at monthly temporal resolution, gridded at 8 km spatial resolution, and covers the period from 1983 to 2013. The NTSG ET data was generated using two approaches. The ET from vegetated land

surface was derived using a modified Penman-Monteith approach with the biome-specific canopy conductance determined from normalised difference vegetation index data, while the open water evaporation was determined using the Priestley-Taylor approach (Zhang et al., 2010). This product has been validated using data from basin-scale water balance calculations in over 200 basins across the globe (Zhang et al., 2010). Additionally, it has been used successfully to evaluate evapotranspiration trends in various regions (Zhang et al., 2009; Mu et al., 2009) and the impacts of vegetation greening and climate change on global ET trends (Zhang et al., 2015).

2.2.4. Water use efficiency

To evaluate the dynamics of ecosystem water use efficiency (WUE), we generated WUE data using the following equation (Cheng et al., 2017):

$$WUE = \frac{GPP}{ET} \qquad Eq\ 1$$

Where WUE is water use efficiency, GPP is gross primary productivity derived using the SCARF model and ET is evapotranspiration data.

2.2.5. Climatic variables

To evaluate the influence of climatic drivers (i.e., precipitation, temperature, and PAR) on the trends in vegetation greening, GPP, ET and WUE, we used independent (data not used to derive GPP, ET and WUE) data (Supplementary Material, Table S2). The precipitation data were derived from the latest version of CHIRPS data (i.e. CHIRPSv2.0) covering the period from 1981 to 2015. The CHIRPSv2.0 data provided rainfall in millimetres at 5 km spatial resolution and at daily, pentad, dekad or monthly temporal resolution (Funk et al., 2015). The air temperature and PAR data were derived from the TERRACLIMATE data produced by the

University of Idaho Climatology Lab (Supplementary Material, Table S2). These are monthly gridded data derived by combining high-spatial resolution climatological normals from the WorldClim dataset, with coarser spatial resolution, but time-varying data from CRU Ts4.0 and the Japanese 55-year Reanalysis (JRA55) (Abatzoglou *et al.,* 2018). The TERRACLIMATE data have been validated using number of station-based observations from a variety of networks including the Global Historical Climate Network, SNOTEL, and RAWS and have been shown to achieve high correlation with *in-situ* data (Abatzoglou *et al.,* 2018).

2.3. Data Analysis

Due to the differences in the spatial resolution of the various datasets and products, all the data were resampled to 0.05 degrees using the aggregate and resample functions (bilinear algorithm) from the R package 'raster' (Hijmans 2021). All resampling processes were computed by snapping the resampled raster to a reference one to ensure that the new resized pixels were perfectly aligned and occupy the same position across the time series. Finally, all the data were reprojected to the same coordinate system (i.e., World Geodetic Survey - WGS 1984 projection). We then calculated per-pixel trends (*slope of linear regression*) of NDVI, Evapotranspiration, Gross Primary Productivity and Water Use Efficiency at an annual time-step from 1982-2015 and determined whether the trends were increasing ($slope > 0$) or decreasing ($slope < 0$) in each pixel. T-test was then used to determine and extract pixels where the observed trends were statistically significant at 95% level ($p\text{-}value\ 0.05$). Additionally, we calculated the annual mean for each of the variables (i.e., NDVI, ET, GPP, and WUE) for the whole region and for the various bioclimatic zones in the region (i.e., arid zone, semi-arid zone, sub humid zone and humid zone) and then evaluated the changes in their magnitude and trend from 1982 to 2015. Finally, we used Person's correlation coefficient to evaluate the spatiotemporal relationship between vegetation greening and GPP, ET, and WUE and the

244 influence of climatic variables (i.e., precipitation, temperature, and PAR) on greening, GPP,
245 ET and WUE.

246

247 **3.0. Results**

248 **3.1. Trends in vegetation greenness, gross primary production, evapotranspiration, and**
249 **water use efficiency**

250 The trend in mean annual NDVI for the whole study area and the various bioclimatic zones
251 had two distinct patterns (Figure 2). The whole region experienced significant positive trend
252 (implying greening) at a rate of *~0.002 NDVI year*$^{-1}$ from 1982 to 2000 (Figure 2a). However,
253 this positive trend diminished from the year 2000 to 2015, with the region experiencing a steady
254 state of greenness (Figure 2a). A similar pattern was observed in the various bioclimatic zones
255 where strong significant positive trends (increase) in NDVI were observed from 1982 to 2000
256 (Figure 2b-e). The strong positive trend in the various bioclimatic zones diminished after the
257 year 2000, with the arid zone experiencing small non-significant negative trend (Figure 2b).

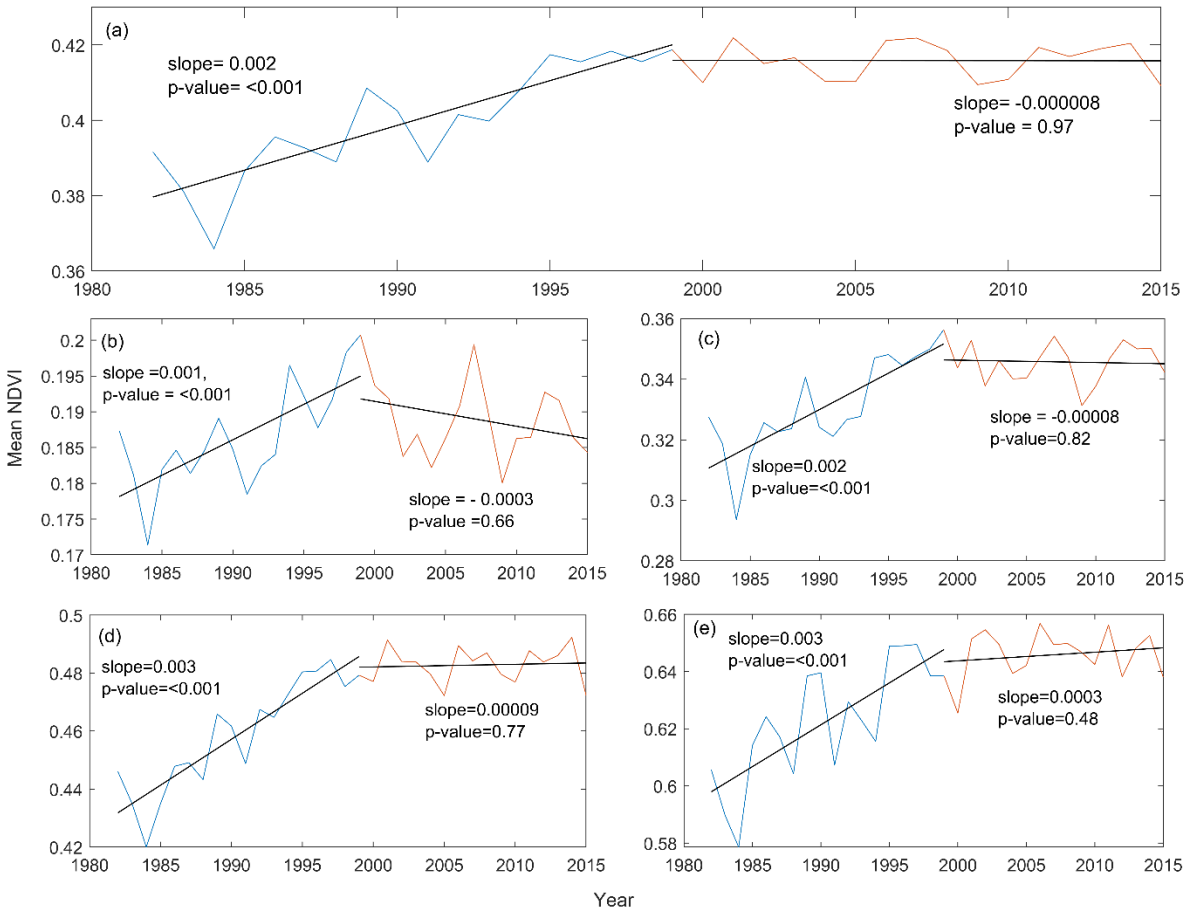

Figure 2: Trends of inter-annual mean NDVI (a) Whole study area, (b) Arid biome, (c) Semi-arid biome, (d) Sub-humid biome, and (e)Humid biome

Similar pattern observed in NDVI was detected in the annual mean GPP trend (Figure 3). The whole region experienced an increase in GPP at a rate of ~ *0.03 PgC per year* from 1982 to 2000 (Figure 3a). Significant positive trends were also observed in the various bioclimatic zones from 1982 to 2000 (Figure 3b-e). However, from the year 2000 to 2015, there was a slight decline in GPP in the whole region and in the various bioclimatic zones (Figure 3). In terms of carbon sequestration potential, the total annual GPP rose from approximately ~*3.9 PgC/year* in 1982 to ~ *4.6 PgC/year* in 2000, resulting in an increase of approximately 17.95%. However, from the year 2000 onwards there was a slight decline in total annual GPP from ~*4.6 PgC/year* in 2000 to ~*4.3 PgC/year* in 2015(Figure 3a).

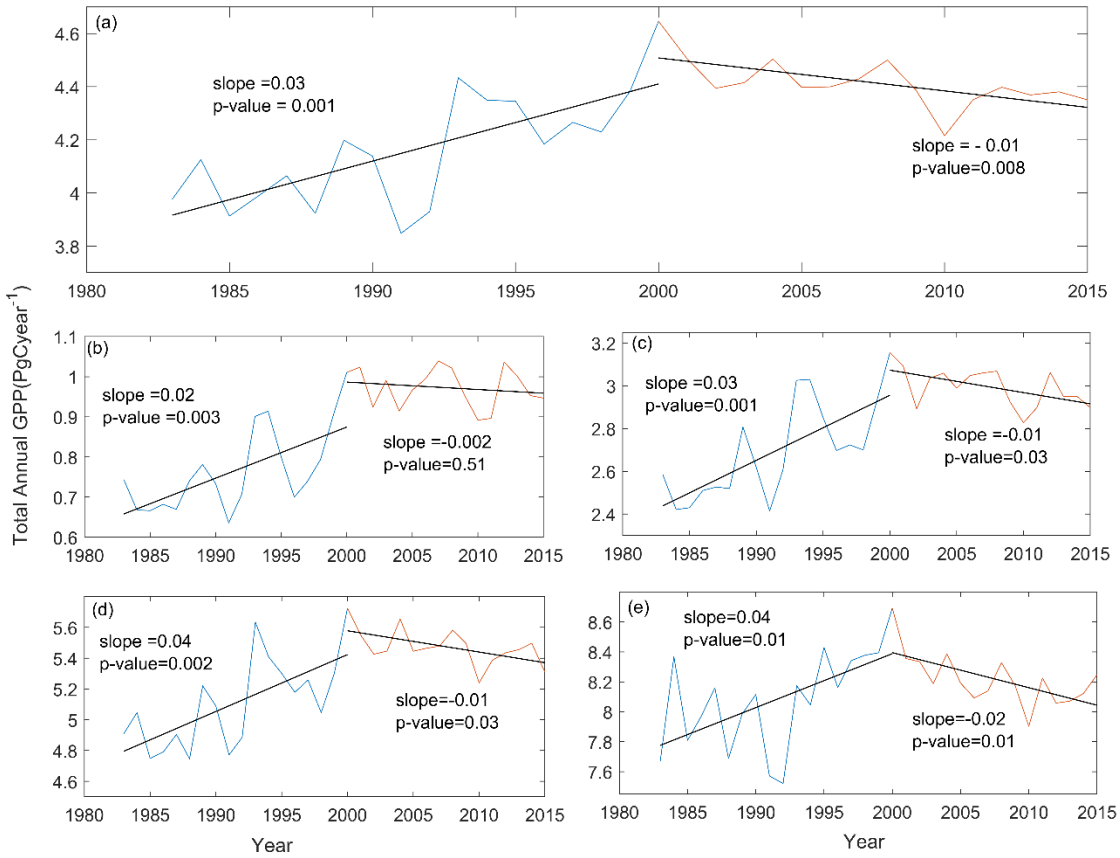

Figure 3: Trends of interannual total GPP (PgCyear^{-1}) for a) Whole study area, b) Arid biome, c) Semi-arid biome, d) Sub-humid biome and e) Humid biome

Unlike the patterns observed in NDVI and GPP, the trend of the mean annual ET showed consistent significant positive trend across the two break-point periods (Figure 4). For the whole region, the trend for ET was 0.3 *mm/year* from 1982 to 2000 and *0.39 mm/year* from 2000 to 2015 (Figure 4a). Similar significant positive trends were observed in the various bioclimatic zones (Figure 4b-e). Over the entire study period, the mean ET increased from *~47 mm/year* to *~57 mm/year,* a *~21.28%* increase.

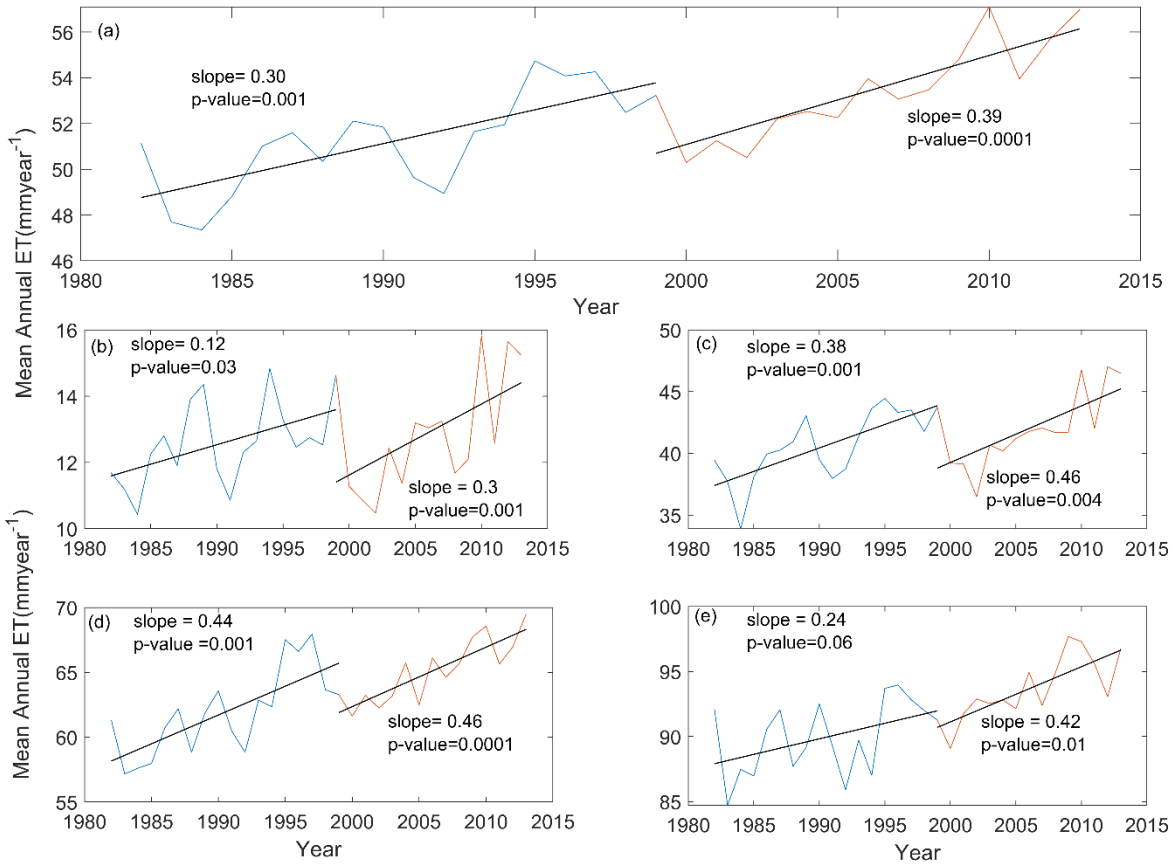

279

280 *Figure 4: Trends of interannual mean ET (mm/year) for a) Whole study area, b) Arid biome, c)*
281 *Semi-arid biome, d) Sub-humid biome and e) Humid biome*

282 The WUE had negative trends in the two distinct break point periods (Figure 5). In the whole
283 region, the WUE experienced a non-significant negative trend at a rate of *-0.005 gC mm^{-1}H2O*
284 *per year* in the first break-point period and a significant negative trend at a rate of *-0.02 gC*
285 *mm^{-1}H2O per year* in the second breakpoint period (Figure 5a). Similar trends were observed
286 in the various bioclimatic zones (Figure 5a-e). It is interesting to note a large increase in WUE
287 between 1999-2000. Looking at the GPP trend (Figure 3) and ET trend (Figure 4), it is
288 noticeable that the GPP continued to increase strongly, while ET reduced during this time.
289 Since WUE is a function of GPP and ET, the increase in GPP and the drop in ET during this
290 time explains the increase in WUE. Prior to this time, the region experienced a strong El-Niño
291 event from 1997-98, which was accompanied by high temperatures and unusually high

precipitation amounts (Anyamba et al., 2002). This was then followed by a period of reduced precipitation during the 1999-2000 La Niña event (Anyamba et al., 2002). This reduction in precipitation during the La Niña period could explain the observed drop in ET. However, the reduction in GPP seemed to have a one-year lag, explaining the continued increase in GPP from 1999-2000.

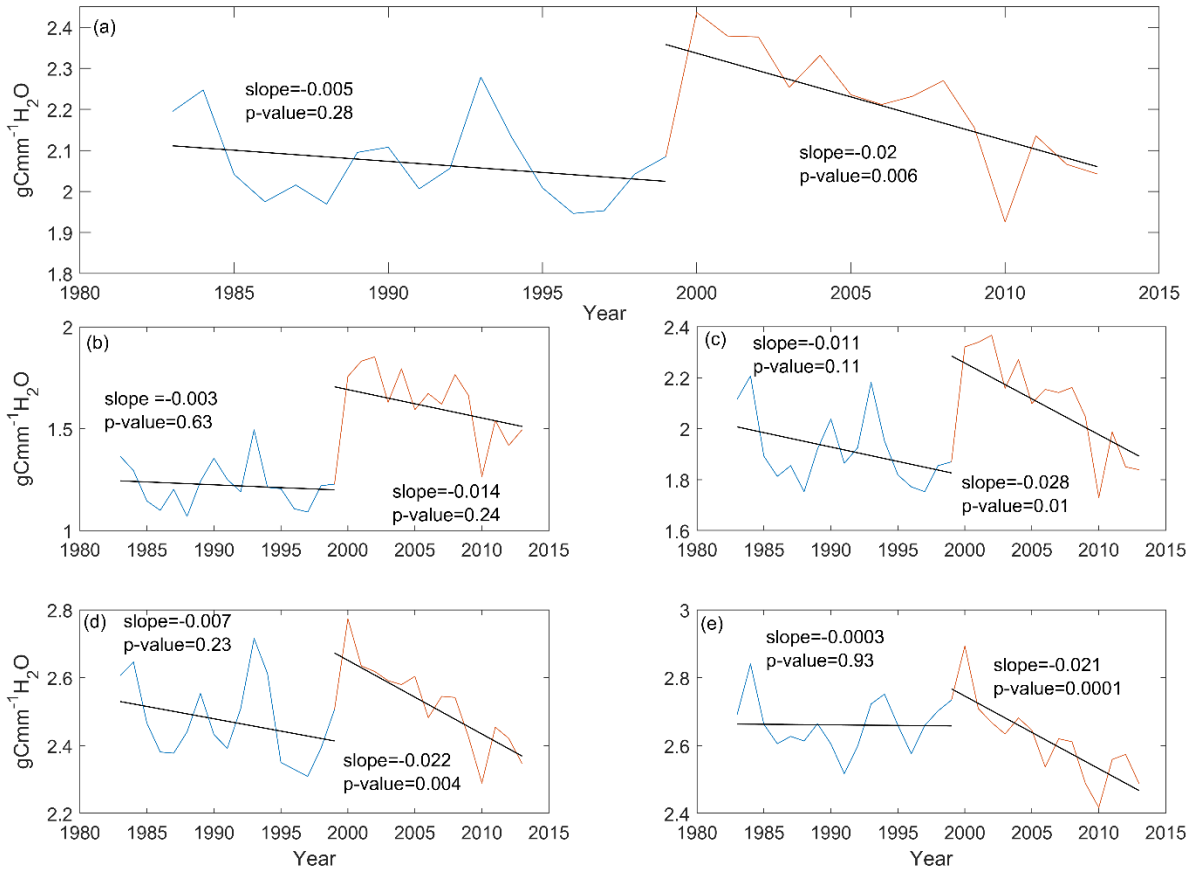

Figure 5: Trends of interannual mean WUE (gC mm$^{-1}H_2O$) for a) Whole study area, b) Arid biome, c) Semi-arid biome, d) Sub-humid biome and e) Humid biome

3.2 Spatial distribution of trends in vegetation greenness, gross primary production, evapotranspiration, and water use efficiency

The positive trends in NDVI (implying vegetation greening) were widespread covering about 60.26% of pixels (~ 5.4 million Km^2) across the region compared to significant negative trends

(0.05% of pixel, ~0.005 million Km^2), implying vegetation browning in the first period of the study (i.e., 1982-2000) (Figure 6a). However, in the second period of the study (i.e., 2000-2015), only 10.47% of pixels (~0.9 million Km^2) experienced positive trends, while 13.19% of pixels (~1.1 million Km^2) experienced negative trends (Figure 7a). Similarly, in the first period of the study there was widespread significant positive trends in GPP (24.37% of pixels, ~2.18 million Km^2), representing increase in carbon sequestration potential, compared to only 2.43% of pixels (~0.2 million Km^2) experiencing significant reduction in GPP (Figure 6b).However, in the second period of the study the areas experiencing positive trends in GPP reduced to 5.46% of pixels (~0.48 million Km^2), whereas the areas experiencing significant negative trends increased to 18.93% of pixels (~1.69 million Km^2) (Figure 7b). The reductions in GPP were mainly located in the humid bioclimatic zone in southern parts of West Africa and in central Ethiopia (Figure 7b). The spatial distribution of ET trends showed an East-West divide, with most of Eastern parts (Horn of Africa i.e., Eritrea, Ethiopia, and Somalia) experiencing negative trends while the Western regions experiencing positive trends (Figure 6c). Overall, in the first period 48.48% of pixels (~ 4.3 million Km^2) had positive trends in ET compared to only 4.48% of the pixels (~0.4 million Km^2) where negative trends were observed (Figure 6c). Similar trends and pattern were observed in the second period of the study with 47.8% of the pixels (~4.28 million Km^2) experiencing positive trends while only 1.4% of pixels (~0.13 million Km^2) experiencing negative trends in ET (Figure 7c). Finally, the distribution of trends in ecosystem WUE showed that the region mainly experienced negative trends in WUE (Figure 6d and 7d). In the first period of the study, 13.55% of pixels (~1.2 million Km^2) mostly located in the western region, experienced negative trends, whereas 8% of pixels (~0.72 million Km^2) mostly located in the eastern region, experienced positive trends in WUE (Figure 6d). However, in the second period of the study, the areas experiencing significant negative trends were

widespread and increased to 38.42% of pixels (~3.4 million Km^2), compared to only 0.98% of pixels (~0.09 million Km^2) experiencing positive trends in WUE (Figure 7d).

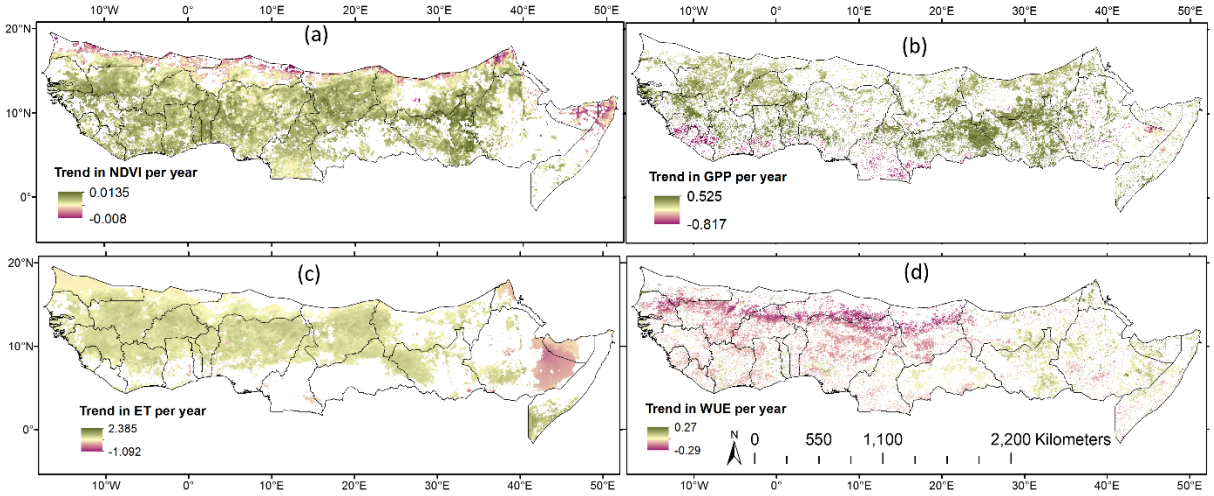

Figure 6: Spatial distribution of areas showing statistically significant (p<0.05) positive and negative trends from 1982-2000 in: a) NDVI, b) GPP c) Evapotranspiration and d) WUE

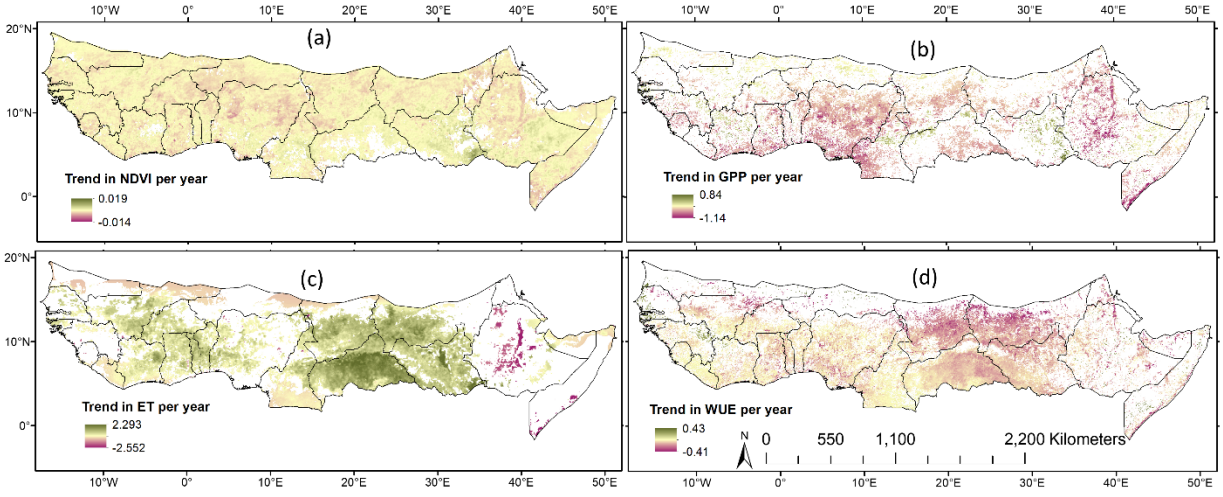

Figure 7: Spatial distribution of areas showing statistically significant (p<0.05) positive and negative trends from 2000-2015 in: a) NDVI, b) GPP c) Evapotranspiration and d) WUE

3.3. Influence of greening on GPP, ET and WUE

The influence of greening (changes in NDVI) on GPP, ET and WUE was evaluated using per-pixel Person's correlation coefficient(r) (Figure 8). Vegetation greening had a strong positive influence on GPP across the whole study area and in the various bioclimatic zones. The strongest correlation between greening and GPP was observed in the semi-arid (*r=0.77, p<0.01*) and sub-humid zones (*r=76, p<0.01*), while the weakest correlation was in the humid zone (*r=0.40, p<0.05*) (Figure 8a). Similarly, greening had a positive influence on ET. Strong positive correlation between greening and ET was observed in semi-arid, sub-humid, and humid bioclimatic zones, while moderate correlation was observed in the arid bioclimatic zone (Figure 8b). Finally, even though there was an increase in WUE with increasing NDVI, their correlation was less obvious (Figure 8c). In the whole study area and the arid zone, there was a low positive correlation between greening and WUE. However, in the semi-arid and sub-humid zones and humid, there was a low to moderate negative correlation between greening and WUE (Figure 8c).

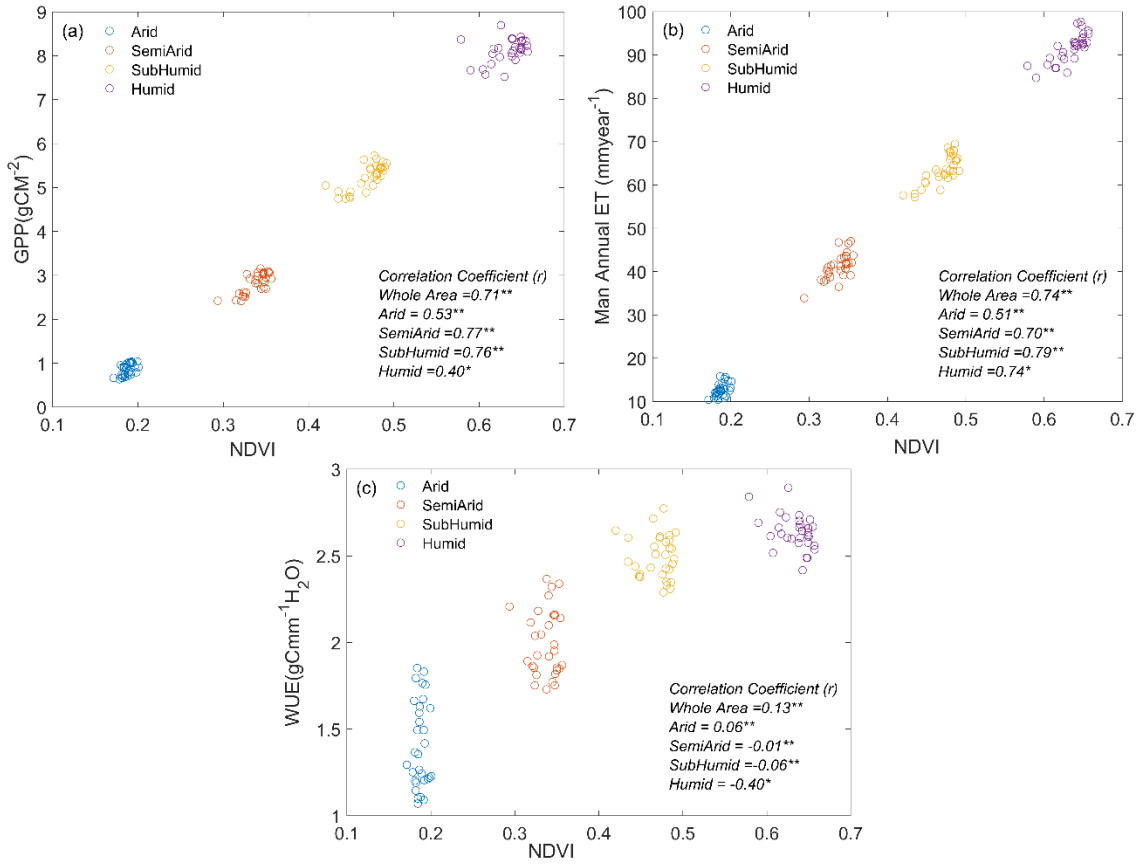

Figure 8: Pearson's correlation between greening (NDVI) and GPP, ET, and WUE *(**p <0.01, *p <0.05*)

3.4. Role of Climate in the dynamics of NDVI, GPP, ET and WUE

Both precipitation and temperature had a positive correlation with NDVI, while PAR had a negative correlation with NDVI in all the bioclimatic zones (Table 1, Figure S2). Precipitation had higher positive correlation with NDVI compared to temperature, highlighting the importance of precipitation in influencing vegetation growth in this region. Indeed, precipitation trend seem to explain the pattern of trend observed in NDVI (that is, the high increase from 1982 to 2000 and then a flattening trend after 2000 in the whole region and in the various biomes) (Figure 9). As expected, the influence of precipitation on NDVI in the arid (*r= 0.76, p<0.01*) and semi-arid (*r=0.74, p<0.01*) regions was higher than in sub-humid (*r=0.55, p<0.01*) and humid (*r=0.49, p<0.05*) zones. Similar to NDVI, precipitation had the strongest correlation with GPP followed by temperature. Even though PAR had a positive correlation with GPP, in most cases this correlation was weak and only significant in the arid zone. Both precipitation and temperature had a positive correlation with ET, while PAR had a negative correlation with ET (probably due to increased absorption of PAR at the top of the atmosphere by increased water vapour- Davin et al.,2007). Similar to NDVI and GPP, precipitation had a stronger influence on ET compared to temperature. The influence of precipitation on ET varied with biome, with the strongest influence experienced in the arid biome. Finally, precipitation and temperature mostly had low negative correlation with WUE, whereas PAR had a significant positive correlation with WUE in all the biomes (Table 1).

Table 1: Correlation coefficient (*r*) between NDVI, GPP, ET, WUE and Climatic variables (PPT, Temp and PAR) (** p<0.01, * p<0.05)

Study Zone	NDVI			GPP			ET			WUE		
	PPT	**Temp**	**PAR**	**PPT**	**Temp**	**PAR**	**PPT**	**Temp**	**PAR**	**PPT**	**Temp**	**PAR**
Whole area	0.63**	0.50**	-0.35*	0.40*	0.27	0.18	0.65**	0.52**	-0.41*	-0.34	-0.17	0.56**
Arid	0.76**	0.27	-0.13	0.62**	0.51**	0.44**	0.74**	0.35	-0.31	-0.01	0.29*	0.43**
Semi-arid	0.74**	0.46**	-0.27	0.44*	0.42*	0.19	0.72**	0.41*	-0.42*	-0.42*	-0.12	0.50**
Sub-humid	0.55**	0.48**	-0.46*	0.37*	0.19	0.09	0.50**	0.43*	-0.33	-0.36*	-0.20	0.56**
Humid	0.49*	0.36**	-0.54**	0.20	0.18	0.03	0.38*	0.54**	-0.46**	-0.19	-0.36*	0.71**

375

376

377 *Figure 9: Comparison of trends in Precipitation and NDVI for (a) Whole study area, (b) Arid*
378 *biome, (c) Semi-arid biome, (d) Sub-humid biome and (e) Humid biome (Solid line: 1982-2000,*
379 *Dashed line: 2000-2015)*

380 The spatial distribution of significant correlation between climatic variables and NDVI indicate
381 that precipitation had strong positive influence on NDVI in arid, semi-arid and dry sub-humid
382 zones (Figure 10a,). Even though widespread positive correlation was observed between
383 temperature and NDVI, the bioclimatic zonal patterns were less defined (Figure 10b). The
384 significant negative influence of PAR on NDVI were mostly in the subhumid and humid zones
385 (Figure 10c). For GPP, precipitation had a strong positive influence in the arid and semi-arid
386 bioclimatic zones (Figure 10d), whereas PAR had strong positive influence in the sub-humid
387 and humid zones (Figure 10f). Similar to NDVI, there was no clear bioclimatic zonal pattern
388 on the influence of temperature on GPP (Figure 10e). Spatial correlations with ET indicate that

precipitation had a strong positive influence on ET in arid and semi-arid zones (Figure 10g), whereas temperature had an East (negative influence) and West (positive influence) divide on its influence on ET (Figure 10h). The negative correlation between PAR and ET was strongest in the arid and semi-arid zones (Figure 10i). We hypothesise that this negative relationship could be linked to higher ET resulting in potential higher water vapour in the atmosphere, which could result in high absorption of incoming solar radiation at the top of the atmosphere, thereby reducing the amount of PAR reaching the ground (Davin et al., 2007). Finally, the spatial distribution of the relationship between climatic variables and WUE indicate that precipitation mainly had a strong negative influence on WUE in the arid and semi-arid zones (Figure 10j), whereas temperature had an East-West divide on its influence on WUE (i.e., western regions had negative correlations, while Eastern regions had positive correlations) (Figure 10k). The positive influence of PAR on WUE was widespread across all the various bioclimatic zones (Figure 10l).

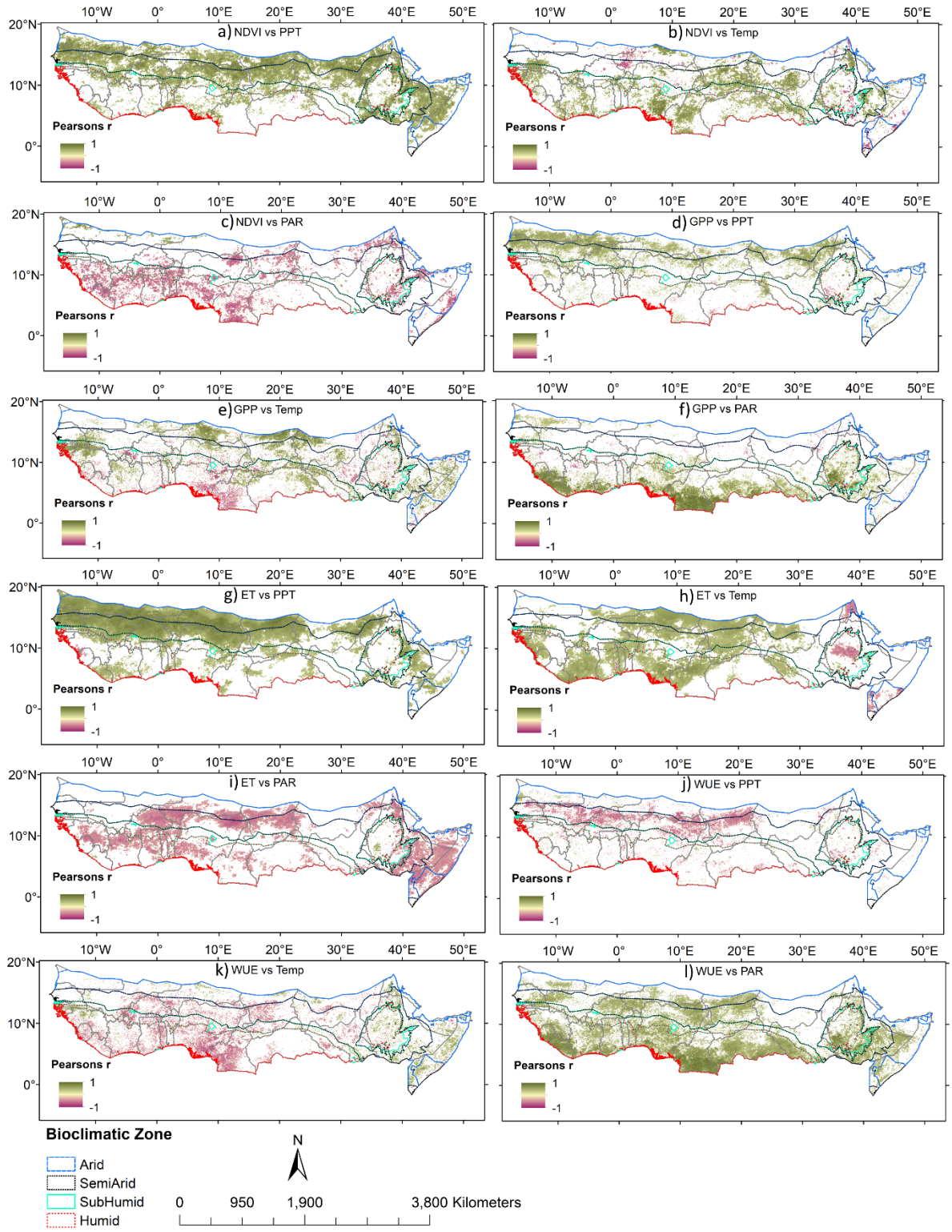

405

406 Figure 10: *Spatial distribution of pixels having statistically significant (p<0.05) positive and*

407 *negative correlation(r) between: NDVI (a-c), GPP(d-f), ET(g-i), WUE (j-l), and climatic*

408 *variables (i.e., Precipitation, Temperature and PAR)*

4. Discussion

Most of the previous studies using Earth Observation data have reported vegetation greening in the Sahel parts of the study area (Ekludh and Olsson, 2003; Hickler et al., 2005; Olsson et al., 2005; Hermann et al., 2005; Fensholt et al., 2012; Dardel et al., 2014; Kaptue et al., 2015). Here we show that this greening was widespread across the African Sahel-Sudano-Guinean region, especially from 1982-2000 (i.e., covering an area of about 5.4 million Km^2). Additionally, the greening occurred across all bioclimatic zones (i.e., arid, semiarid, sub-humid and humid). Furthermore, we show that the rate of vegetation greening slowed after the year 2000, with only an area of approximately 0.9 million K^2 experiencing greening from 2000 to 2015. Several explanations have been given on the causes of greening found particularly in the Sahel including wetter conditions (Haarsma *et al.,* 2005; Kaptue *et al.,* 2015; Brandt *et al.,* 2016); carbon dioxide fertilisation (Bathiany *et al.,* 2014; Traore *et al.,* 2014; Lu et al., 2016); human-induced land use change and woody vegetation encroachment particularly in savanna ecosystems (Brandt *et al.,* 2015; Brandt *et al.,* 2016; Venter *et al.,* 2018; Anchang *et al.,* 2019). Our results confirm that in the wider region, the vegetation greening was largely controlled by increase in precipitation, with the strongest influence occurring in the arid, semi-arid and subhumid climatic zones, where water availability is a key limiting factor for vegetation growth. Indeed, the reduction in the rate of vegetation greening after the year 2000 was associated with a reduction and stabilisation of precipitation observed from the year 2000 onwards (Figure 9). Fewer areas (~0.005 million Km^2) had negative greening trends prior to the year 2000, representing vegetation browning. However, vegetation browning increased slightly to ~1.1 million Km^2 between 2000-2015 The areas where vegetation browning occurred were mainly located in and around major settlements (e.g., areas around Bamako in Mali; Khartoum in Sudan and Addis Ababa) and the cropland belt in Ethiopia, supporting the findings that human activities play a major role in the reduction of vegetation cover (Brandt et al., 2017).

Even though information on relative measures of ecosystem changes such as vegetation greenness is important when investigating the causes of such change, absolute measures such as vegetation productivity (e.g., grams of carbon per unit area per unit time) are more important when quantifying the dynamics of ecosystem services such as changes in the global carbon cycle (Le Quere et al., 2015; Ardo et al., 2018). Here we used a light use efficiency model (i.e., the SCARF model, Ogutu et al., 2013) to show that the vegetation greening had resulted in an increase of about 17.95% in carbon sequestration potential (GPP) (from *~3.9 PgC/year* in 1982 to *~4.6 PgC/year* in the 2000) of the Sahel-Sudano-Guinean region. These results are in line with a study by Brandt et al., (2015), which reported increase in biomass in parts of the Sahel-Sudano-Guinean region due to vegetation greening. After the year 2000 there was a slight decrease in GPP, in line with the changes in vegetation greening and reduction in precipitation. Similar to vegetation greening, precipitation had the strongest influence on GPP. As expected, this influence was stronger in drier arid and semi-arid zones, where water availability is critical in vegetation productivity, compared to sub-humid and humid zones. In African drylands, the carbon cycle dynamics is often dominated by seasonal changes in herbaceous vegetation (influenced by rainfall patterns and wildfire events) (Williams *et al.,* 2007). This makes carbon stocks or pool in this region to be relatively labile (i.e., due to the seasonality of herbaceous vegetation, wildfires, and the frequent occurrence of extreme climatic events like droughts) (Bond and Keeley, 2005; Williams et al., 2007). However, studies evaluating the characteristics of vegetation greening in the Sahel-Sudano-Guinean region have reported woody encroachment as the main cause of vegetation greening in the region (Brandt et al., 2015; Brandt et al., 2016). This change in vegetation composition imply that the carbon stock in this region may become less labile and the increase in carbon sequestration potential observed in this study is likely to be sustained since woody vegetation has more permanence compared to the seasonal herbaceous vegetation. Therefore, the changes in carbon sequestration potential

observed in this study is likely to have a long-lasting impact on the carbon cycle of the region. For example, the increase in productivity by ~0.7 PgC/year reported from 1982-2000 in this study is slightly higher than the ~0.4 PgC/year carbon emission per year that has been attributed to land use change (particularly from deforestation) in Africa (Haughton 2003; Williams et al., 2007). If it is assumed that about half of the carbon (i.e., ~0.35 PgC/year in this study) captured through photosynthesis is sequestered due the permanence of woody vegetation, then the increase in productivity due to the vegetation greening could offset substantial amounts of carbon emissions due to land use change in Africa, thereby influencing the dynamics of carbon cycle in the region. Additionally, studies by Poulter et al., (2014) and Ahlstrom et al., (2015) already showed that, contrary to earlier assertions, drylands are dominant contributors to changes in the global carbon sink over time, contributing up to 57 % of the positive trend in global carbon sink, while also playing a major role in driving the inter-annual anomaly of terrestrial ecosystems global carbon sinks. Our results reinforce these findings by showing that drylands undergoing vegetation greening, particularly those dominated by woody encroachment, are likely to become major contributors to the global carbon sink due to the potential alteration of the labile nature of carbon stocks in these drylands.

Since changes in vegetation growth in drylands are likely to affect the water cycle, we evaluated the relationship between the observed greening and the ET and WUE of the region. Our results showed that there was a strong relationship between greening and increase in ET across all the bioclimatic zones. The presence of woody vegetation, which has been shown to be the main cause of greening in this region (Brandt et al., 2015; Brandt et al., 2016; Venter et al., 2018), can lead to lowering of albedo, greater surface roughness, and greater rooting depth (i.e., increasing access to soil moisture), which would result in the observed increased ET (Lawrence and Vandecar, 2015; Spracklen *et al.,* 2018). The evaluation of the influence of climatic variables on ET, showed that precipitation and temperature had significant influence on ET.

Increases in precipitation would lead to more water availability and increases in temperature would result in more evapotranspiration, hence the strong correlation observed between ET and the two climatic variables. Even though precipitation had a major influence on vegetation greening and ET, it is worth nothing that the reverse is also possible. That is, vegetation greening (especially woody encroachment), can lead to alteration of surface albedo, surface roughness and access to soil moisture, which would result in increased ET and hence increased precipitation as per the hydrological cycle (Lawrence and Vandecar, 2015; Spracklen *et al.,* 2018). Our results are in line with previous studies have reported that, where water is not limiting, vegetation greening has led to increases in ET (Zhang et al 2015). Additionally, other global studies have also reported significant increases in global evapotranspiration over the last few decades, attributed to both greening and changes in precipitation levels (Zhang et al., 2015; Zhang et al., 2016).

The analysis of the dynamics of WUE indicated that, overall, the region experienced negative trends in WUE, implying a reduction in the amount of carbon fixed per unit water used. Since WUE is calculated as a ratio between GPP and ET, this result implies that even though there was an increase in GPP, the increase in ET was at a much higher rate, thereby resulting in a reduction in WUE. Even though the overall trend in WUE was negative, analysis of the spatial temporal distribution of significant trends in WUE showed a clear East-West pattern. The Horn of Africa mostly experienced positive trends, while western parts of the Sahel-Sudano-Guinean region mostly had negative trends in WUE. The explanation for this regional difference can be linked to the dynamics in precipitation. While most of western Sahel-Sudano-Guinean region experienced positive rainfall anomalies from 1980s onwards (Biasutti and Giannini, 2006; Giannini et al., 2013; Dong and Sutton, 2015), the Horn of Africa continued to have negative rainfall anomalies during this period (Nicholson, 2014; Lyon 2014). Therefore, in western Sahel-Sudano-Guinean region, the increase in precipitation coupled with vegetation greening

resulted in a larger magnitude of increase in ET compared to the increase in GPP, resulting in the reduction in WUE. However, in the Horn of Africa, the negative anomaly in precipitation seems to have resulted in vegetation adapting by reducing the rates of ET, while maximising their GPP. Studies have shown that drought conditions tended to increase WUE of vegetation in drylands (e.g., Liu et al., 2015; Ahmadi et al., 2019). This is because vegetation in dry areas often maintain a high GPP to evapotranspiration ratio as an adaptation strategy (Hu et al., 2008; Liu et al., 2015). Global scale studies on the dynamics of WUE have reported an increase in global water use efficiency since the mid-1990s (Cheng et al., 2017). However, the current study show that these increases are not uniform and regional disparities exist.

Even though this study has highlighted the trends in vegetation greening, gross primary productivity, ET, and water use efficiency in the Sahel-Sudano-Guinean region from 1982 to 2015, there are a few limitations in the study. Firstly, we used correlation to evaluate the relationship between climatic variables and the observed trends. However, for such an observational study, there is no way of deciding whether the correlation imply causation. Secondly, when analysing the trend in the time series data, we did not decompose the time series to different components (e.g., trend, seasonality, and noise). Therefore, there may be residual seasonality and noise in the data, which may introduce uncertainty in the results. Finally, the original datasets were in different spatial and temporal resolutions. Aggregating these data through temporal and spatial resampling probably led so some information loss and smoothing of the data thereby introducing some uncertainties in the results.

5. Conclusion

This study revealed widespread vegetation greening in the Sahel-Sudano-Guinean region that was mainly driven by precipitation. Even though the rate of vegetation greening reduced after

the year 2000, the levels of greenness did not revert to pre-greening levels of 1980s, implying a persistent ecosystem change in the region. The vegetation greening resulted in changes in the carbon sequestration potential and the water cycle. Both GPP and ET experienced increases, while WUE reduced over time. The sustained increase in GPP show that, despite factors that often lead to depletion of carbon sequestration in drylands such as rapid litter decomposition and frequent fires, the Sahel-Sudano-Guinean region had become more productive. On the other hand, the vegetation greening and increases in ET has the potential to alter the surface energy balance and the region's water cycle. The overall negative trend in WUE was mainly attributed to a larger increase in ET compared to the moderate increase in GPP. However, regional difference existed in WUE trend, with the Horn of Africa, which has had a sustained negative precipitation anomaly experiencing increase in WUE, while western Sahel-Sudano-Guinean region, which has had a persistent positive precipitation anomaly, experiencing reduction in WUE.

Currently, there is a lack of consensus on the magnitude of the contribution of drylands to the global carbon and water cycle. Our study shows that drylands undergoing ecosystem change (e.g., greening), coupled with climate change, may become important contributors to the global carbon budget and water cycle. Until now most policies focused on mitigating global warming and climate change have focussed on the role of forests in mitigating climate change. However, findings from this study show that drylands could also play an important role in mitigating carbon dioxide build-up in the atmosphere and global warming.

Acknowledgements

We would like to acknowledge the data providers including: the NASA GIMMS group for the NDVI3g.v1 dataset, the ESA CCI for the Land cover data, CARBOAFRICA for the flux tower data, FAO for the aridity index maps, Climate Hazard Centre for CHIRPS data, National Terradynamic Simulation Group (NTSG), University of Montana for the Evapotranspiration data, the University of Delaware for Temperature data, Climatology Lab at the University of Idaho for the VPD, PAR, temperature data, EUMETSAT for the solar radiation data, and the Centre for Global Change Data Processing and Analysis of Beijing Normal University, Beijing, China for the GLASS AVHRR FAPAR data.

Author Contributions

B.O.O conceived the idea of the paper and wrote the initial manuscript, J.D. contributed ideas to the study methodology, F.D. helped with data pre-processing. All authors reviewed the manuscript.

Competing Interests

The authors declare no competing interests

Data Availability

All data used in the paper are freely available from the following sites:

Air temperature data: *https://psl.noaa.gov/data/gridded/data.UDel_AirT_Precip.html*-
(Accessed 04/08/2020)

GLASS FAPAR data: *http://www.glass.umd.edu/FAPAR/AVHRR/* (Accessed on 04/08/2020)

GIMMS NDVI data: *https://ecocast.arc.nasa.gov/data/pub/gimms/3g.v1/* - (Accessed on 04/08/2020)

CHIRPS Precipitation data : *https://data.chc.ucsb.edu/products/CHIRPS-2.0/* - (Accessed on 04/08/2020)

Vapour Pressure Deficit data: *http://www.climatologylab.org/terraclimate.html* (Accessed 04/08/2020)

Solar radiation data: *https://navigator.eumetsat.int/search?query=solar%20r* (Accessed 04/06/2020)

Evapotranspiration data : http://files.ntsg.umt.edu/data/ET_global_monthly/ (Accessed on 04/08/2020)

Land cover data: https://www.esa-landcover-cci.org/ (Accessed on 04/08/2020)

601 **References**

602 Abatzoglou, J. T., Dobrowski, S. Z., Parks, S. A., & Hegewisch, K. C. (2018). TerraClimate,
603 a high-resolution global dataset of monthly climate and climatic water balance from
604 1958–2015. *Scientific data, 5*, 170191.

605 Abdi, A. M., Seaquist, J., Tenenbaum, D. E., Eklundh, L., & Ardö, J. (2014). The supply and
606 demand of net primary production in the Sahel. *Environmental Research Letters, 9*(9),
607 094003.

608 Ahlström, A., Raupach, M. R., Schurgers, G., Smith, B., Arneth, A., Jung, M., . . . Jain, A. K.
609 (2015). The dominant role of semi-arid ecosystems in the trend and variability of the
610 land CO2 sink. *Science, 348*(6237), 895-899.

611 Ahmadi, B., Ahmadalipour, A., Tootle, G., & Moradkhani, H. (2019). Remote Sensing of
612 Water Use Efficiency and Terrestrial Drought Recovery across the Contiguous United
613 States. *Remote Sensing, 11*(6), 731.

614 Ali, A., & Lebel, T. (2009). The Sahelian standardized rainfall index revisited. *International*
615 *Journal of Climatology, 29*(12), 1705-1714.

616 Anchang, J. Y., Prihodko, L., Kaptué, A. T., Ross, C. W., Ji, W., Kumar, S. S., . . . Hanan, N.
617 P. (2019). Trends in Woody and Herbaceous Vegetation in the Savannas of West
618 Africa. *Remote Sensing, 11*(5), 576.

619 Anyamba, A., Tucker, C. J., & Mahoney, R. (2002). From El Niño to La Niña: Vegetation
620 response patterns over east and southern Africa during the 1997–2000 period. *Journal*
621 *of Climate, 15*(21), 3096-3103.

622 Ardö, J., Tagesson, T., Jamali, S., & Khatir, A. (2018). MODIS EVI-based net primary
623 production in the Sahel 2000–2014. *International journal of applied earth*
624 *observation and geoinformation, 65*, 35-45.

625 Bathiany, S., Claussen, M., & Brovkin, V. (2014). CO2-induced Sahel greening in three
626 CMIP5 Earth system models. *Journal of Climate, 27*(18), 7163-7184.
627 Bi, J., Xu, L., Samanta, A., Zhu, Z., & Myneni, R. (2013). Divergent arctic-boreal vegetation
628 changes between North America and Eurasia over the past 30 years. *Remote Sensing,*
629 *5*(5), 2093-2112.
630 Biasutti, M., & Giannini, A. (2006). Robust Sahel drying in response to late 20th century
631 forcings. *Geophysical Research Letters, 33*(11).
632 Bond, W.J. and Keeley, J.E., (2005). Fire as a global 'herbivore': the ecology and evolution
633 of flammable ecosystems. *Trends in ecology & evolution*, 20(7), pp.387-394.
634 Brandt, M., Hiernaux, P., Rasmussen, K., Mbow, C., Kergoat, L., Tagesson, T., . . . Fensholt,
635 R. (2016). Assessing woody vegetation trends in Sahelian drylands using MODIS
636 based seasonal metrics. *Remote sensing of environment, 183*, 215-225.
637 Brandt, M., Mbow, C., Diouf, A. A., Verger, A., Samimi, C., & Fensholt, R. (2015). Ground-
638 and satellite-based evidence of the biophysical mechanisms behind the greening
639 Sahel. *Global Change Biology, 21*(4), 1610-1620.
640 Brandt, M., Rasmussen, K., Peñuelas, J., Tian, F., Schurgers, G., Verger, A., . . . Fensholt, R.
641 (2017). Human population growth offsets climate-driven increase in woody
642 vegetation in sub-Saharan Africa. *Nature ecology & evolution, 1*(4), 0081.
643 Cheng, L., Zhang, L., Wang, Y.-P., Canadell, J. G., Chiew, F. H. S., Beringer, J., . . . Zhang,
644 Y. (2017). Recent increases in terrestrial carbon uptake at little cost to the water cycle.
645 *Nature communications, 8*(1), 110.
646 Chiwara, P., Ogutu, B. O., Dash, J., Milton, E. J., Ardö, J., Saunders, M., & Nicolini, G.
647 (2018). Estimating terrestrial gross primary productivity in water limited ecosystems
648 across Africa using the Southampton Carbon Flux (SCARF) model. *Science of the*
649 *Total Environment, 630*, 1472-1483.

650 Dardel, C., Kergoat, L., Hiernaux, P., Mougin, E., Grippa, M., & Tucker, C. J. (2014). Re-
651 greening Sahel: 30 years of remote sensing data and field observations (Mali, Niger).
652 *Remote sensing of environment, 140*, 350-364.
653 Davin, E.L., de Noblet‐Ducoudré, N. and Friedlingstein, P., (2007). Impact of land cover
654 change on surface climate: Relevance of the radiative forcing concept. *Geophysical*
655 *Research Letters, 3*4(13).
656 Dong, B., & Sutton, R. (2015). Dominant role of greenhouse-gas forcing in the recovery of
657 Sahel rainfall. *Nature Climate Change, 5*(8), 757.
658 Eklundh, L., & Olsson, L. (2003). Vegetation index trends for the African Sahel 1982–1999.
659 *Geophysical Research Letters, 30*(8).
660 Endris, H. S., Lennard, C., Hewitson, B., Dosio, A., Nikulin, G., & Artan, G. A. (2019).
661 Future changes in rainfall associated with ENSO, IOD and changes in the mean state
662 over Eastern Africa. *Climate Dynamics, 52*(3-4), 2029-2053.
663 Fensholt, R., Langanke, T., Rasmussen, K., Reenberg, A., Prince, S. D., Tucker, C., . . .
664 Eastman, R. (2012). Greenness in semi-arid areas across the globe 1981–2007—an
665 Earth Observing Satellite based analysis of trends and drivers. *Remote sensing of*
666 *environment, 121*, 144-158.
667 Funk, C., Peterson, P., Landsfeld, M., Pedreros, D., Verdin, J., Shukla, S., . . . Hoell, A.
668 (2015). The climate hazards infrared precipitation with stations—a new
669 environmental record for monitoring extremes. *Scientific data, 2*(1), 1-21.
670 Giannini, A., Salack, S., Lodoun, T., Ali, A., Gaye, A. T., & Ndiaye, O. (2013). A unifying
671 view of climate change in the Sahel linking intra-seasonal, interannual and longer
672 time scales. *Environmental Research Letters, 8*(2), 024010.
673 Haarsma, R. J., Selten, F. M., Weber, S. L., & Kliphuis, M. (2005). Sahel rainfall variability
674 and response to greenhouse warming. *Geophysical Research Letters, 32*(17).

675 Hein, L., & De Ridder, N. (2006). Desertification in the Sahel: a reinterpretation. *Global*
676 *Change Biology, 12*(5), 751-758.
677 Herrmann, S. M., Anyamba, A., & Tucker, C. J. (2005). Recent trends in vegetation
678 dynamics in the African Sahel and their relationship to climate. *Global Environmental*
679 *Change, 15*(4), 394-404.
680 Herrmann, S. M., & Tappan, G. G. (2013). Vegetation impoverishment despite greening: A
681 case study from central Senegal. *Journal of Arid Environments, 90*, 55-66.
682 Herrmann, S.M., Brandt, M., Rasmussen, K. and Fensholt, R., (2020). Accelerating land
683 cover change in West Africa over four decades as population pressure increased.
684 *Communications Earth & Environment*, 1(1), 1-10.
685 Hickler, T., Eklundh, L., Seaquist, J. W., Smith, B., Ardö, J., Olsson, L., . . . Sjöström, M.
686 (2005). Precipitation controls Sahel greening trend. *Geophysical Research Letters,*
687 *32*(21).
688 Hijmans, R.J., (2021). GeographicDataAnalysisandModeling.*Rpackagerasterversion3.*
689 *4-10.*
690 Houghton, R. A. (2003). Revised estimates of the annual net flux of carbon to the atmosphere
691 from changes in land use and land management 1850–2000. *Tellus B, 55*(2), 378-390.
692 Hu, Z., Yu, G., Fu, Y., Sun, X., Li, Y., Shi, P., . . . Zheng, Z. (2008). Effects of vegetation
693 control on ecosystem water use efficiency within and among four grassland
694 ecosystems in China. *Global Change Biology, 14*(7), 1609-1619.
695 Huang, M., Piao, S., Sun, Y., Ciais, P., Cheng, L., Mao, J., . . . Wang, Y. (2015). Change in
696 terrestrial ecosystem water-use efficiency over the last three decades. *Global Change*
697 *Biology, 21*(6), 2366-2378.
698 Ibrahim, F. N. (1988). Causes of the famine among the rural population of the Sahelian zone
699 of the Sudan. *GeoJournal, 17*(1), 133-141.

Ibrahim, Y. Z., Balzter, H., & Kaduk, J. (2018). Land degradation continues despite greening in the Nigeria-Niger border region. *Global Ecology and Conservation, 16*,

Kandji, S. T., Verchot, L., & Mackensen, J. (2006). Climate change and variability in the Sahel region: impacts and adaptation strategies in the agricultural sector. In: World Agroforestry Centre Nairobi, Kenya.

Kaptué, A. T., Prihodko, L., & Hanan, N. P. (2015). On regreening and degradation in Sahelian watersheds. *Proceedings of the National Academy of Sciences, 112*(39), 12133-12138.

Keenan, T. F., Hollinger, D. Y., Bohrer, G., Dragoni, D., Munger, J. W., Schmid, H. P., & Richardson, A. D. (2013). Increase in forest water-use efficiency as atmospheric carbon dioxide concentrations rise. *Nature, 499*(7458), 324.

Kent, C., Chadwick, R., & Rowell, D. P. (2015). Understanding uncertainties in future projections of seasonal tropical precipitation. *Journal of Climate, 28*(11), 4390-4413.

Lawrence, D. and Vandecar, K., (2015). Effects of tropical deforestation on climate and agriculture. *Nature climate change*, 5(1), pp.27-36.

Le Quéré, C., Moriarty, R., Andrew, R. M., Peters, G. P., Ciais, P., Friedlingstein, P., . . . Arneth, A. (2015). Global carbon budget 2014. *Earth System Science Data, 7*(1), 47-85.

Liu, Y., Xiao, J., Ju, W., Zhou, Y., Wang, S., & Wu, X. (2015). Water use efficiency of China's terrestrial ecosystems and responses to drought. *Scientific reports, 5*, 13799.

Lu, X., Wang, L., & McCabe, M. F. (2016). Elevated CO 2 as a driver of global dryland greening. *Scientific reports, 6*, 20716.

Lyon, B. (2014). Seasonal drought in the Greater Horn of Africa and its recent increase during the March–May long rains. *Journal of Climate, 27*(21), 7953-7975.

724 Mu, Q., Jones, L. A., Kimball, J. S., McDonald, K. C., & Running, S. W. (2009). Satellite
725 assessment of land surface evapotranspiration for the pan-Arctic domain. *Water*
726 *Resources Research, 45*(9).
727 Neely, C., Bunning, S. and Wilkes, A., (2009). Review of evidence on drylands pastoral
728 systems and climate change. Rome: FAO.
729 Nicholson, S. E. (2009). A revised picture of the structure of the "monsoon" and land ITCZ
730 over West Africa. *Climate Dynamics, 32*(7-8), 1155-1171.
731 Nicholson, S. E. (2013). The West African Sahel: A review of recent studies on the rainfall
732 regime and its interannual variability. *ISRN Meteorology, 2013*.
733 Nicholson, S. E. (2014). A detailed look at the recent drought situation in the Greater Horn of
734 Africa. *Journal of Arid Environments, 103*, 71-79.
735 Nicholson, S. E., Tucker, C. J., & Ba, M. B. (1998). Desertification, drought, and surface
736 vegetation: An example from the West African Sahel. *Bulletin of the American*
737 *Meteorological Society, 79*(5), 815-830.
738 Ogutu, B. O., Dash, J., & Dawson, T. P. (2013). Developing a diagnostic model for
739 estimating terrestrial vegetation gross primary productivity using the photosynthetic
740 quantum yield and Earth Observation data. *Global Change Biology, 19*(9), 2878-
741 2892.
742 Olsson, L., Eklundh, L., & Ardö, J. (2005). A recent greening of the Sahel—trends, patterns,
743 and potential causes. *Journal of Arid Environments, 63*(3), 556-566.
744 Pinzon, J., & Tucker, C. (2014). A non-stationary 1981–2012 AVHRR NDVI3g time series.
745 *Remote Sensing, 6*(8), 6929-6960.
746 Pinzon, J. E., Brown, M. E., & Tucker, C. J. (2005). Hilbert-Huang transform and its
747 applications. *Interdisciplinary mathematical sciences, 5*, 311.

748 Poulter, B., Frank, D., Ciais, P., Myneni, R. B., Andela, N., Bi, J., . . . Liu, Y. Y. (2014).
749 Contribution of semi-arid ecosystems to interannual variability of the global carbon
750 cycle. *Nature, 509*(7502), 600.
751 Prince, S. D., De Colstoun, E. B., & Kravitz, L. L. (1998). Evidence from rain-use
752 efficiencies does not indicate extensive Sahelian desertification. *Global Change*
753 *Biology, 4*(4), 359-374.
754 Reichstein, M., Falge, E., Baldocchi, D., Papale, D., Aubinet, M., Berbigier, P., Bernhofer,
755 C., Buchmann, N., Gilmanov, T., Granier, A. and Grünwald, T., (2005). On the
756 separation of net ecosystem exchange into assimilation and ecosystem respiration:
757 review and improved algorithm. *Global change biology*, 11(9), pp.1424-1439.
758 Rowell, D. P., Senior, C. A., Vellinga, M., & Graham, R. J. (2016). Can climate projection
759 uncertainty be constrained over Africa using metrics of contemporary performance?
760 *Climatic Change, 134*(4), 621-633.
761 Sinclair, A. R. E., & Fryxell, J. M. (1985). The Sahel of Africa: ecology of a disaster.
762 *Canadian Journal of Zoology, 63*(5), 987-994. doi:10.1139/z85-147
763 Spracklen, D.V., Baker, J.C.A., Garcia-Carreras, L. and Marsham, J.H., (2018). The effects
764 of tropical vegetation on rainfall. *Annual Review of Environment and Resources*. 43:1,
765 193-218
766 Thomas, D. S. G., & Middleton, N. J. (1994). *Desertification: exploding the myth*: John
767 Wiley and Sons.
768 Tietjen, B., Jeltsch, F., Zehe, E., Classen, N., Groengroeft, A., Schiffers, K., & Oldeland, J.
769 (2010). Effects of climate change on the coupled dynamics of water and vegetation in
770 drylands. *Ecohydrology: Ecosystems, Land and Water Process Interactions,*
771 *Ecohydrogeomorphology, 3*(2), 226-237.

772 Traore, A. K., Ciais, P., Vuichard, N., Poulter, B., Viovy, N., Guimberteau, M., . . . Fisher, J.
773 B. (2014). Evaluation of the ORCHIDEE ecosystem model over Africa against 25
774 years of satellite-based water and carbon measurements. *Journal of Geophysical*
775 *Research: Biogeosciences, 119*(8), 1554-1575.
776 United Nations Conference on, D. (1977). *Desertification: its causes and consequences* (Vol.
777 1): Pergamon.
778 Venter, Z.S., Cramer, M.D. and Hawkins, H.J., (2018). Drivers of woody plant encroachment
779 over Africa. *Nature communications*, 9(1), pp.1-7.
780 Williams, C. A., Hanan, N. P., Neff, J. C., Scholes, R. J., Berry, J. A., Denning, A. S., &
781 Baker, D. F. (2007). Africa and the global carbon cycle. *Carbon balance and*
782 *management, 2*(1), 3.
783 Yang, Y., Guan, H., Batelaan, O., McVicar, T. R., Long, D., Piao, S., . . . Simmons, C. T.
784 (2016). Contrasting responses of water use efficiency to drought across global
785 terrestrial ecosystems. *Scientific reports, 6*, 23284.
786 Zhang, K., Kimball, J. S., Mu, Q., Jones, L. A., Goetz, S. J., & Running, S. W. (2009).
787 Satellite based analysis of northern ET trends and associated changes in the regional
788 water balance from 1983 to 2005. *Journal of Hydrology, 379*(1-2), 92-110.
789 Zhang, K., Kimball, J. S., Nemani, R. R., & Running, S. W. (2010). A continuous satellite-
790 derived global record of land surface evapotranspiration from 1983 to 2006. *Water*
791 *Resources Research, 46*(9).
792 Zhang, K., Kimball, J. S., Nemani, R. R., Running, S. W., Hong, Y., Gourley, J. J., & Yu, Z.
793 (2015). Vegetation greening and climate change promote multidecadal rises of global
794 land evapotranspiration. *Scientific reports, 5*, 15956.

795 Zhang, Y., Peña-Arancibia, J. L., McVicar, T. R., Chiew, F. H. S., Vaze, J., Liu, C., . . . Liu,
796 Y. Y. (2016). Multi-decadal trends in global terrestrial evapotranspiration and its
797 components. *Scientific reports, 6*, 19124.
798 Zheng, H., Lin, H., Zhou, W., Bao, H., Zhu, X., Jin, Z., . . . Tang, Y. (2019). Revegetation
799 has increased ecosystem water-use efficiency during 2000–2014 in the Chinese Loess
800 Plateau: Evidence from satellite data. *Ecological Indicators, 102*, 507-518.
801 Zhou, S., Yu, B., Schwalm, C. R., Ciais, P., Zhang, Y., Fisher, J. B., . . . Huntzinger, D. N.
802 (2017). Response of water use efficiency to global environmental change based on
803 output from terrestrial biosphere models. *Global Biogeochemical Cycles, 31*(11),
804 1639-1655.
805